



www.sciencemag.org/cgi/content/full/1181661/DC1

Supporting Online Material for

On the Origin of Species by Natural and Sexual Selection

G. Sander van Doorn,* Pim Edelaar, Franz. J. Weissing

*To whom correspondence should be addressed. E-mail: sander.vandoorn@iee.unibe.ch

Published 26 November 2009 on *Science Express*

DOI: 10.1126/science.1181661

This PDF file includes:

SOM Text

Figs. S1 to S3

References and Notes

Supporting online material

1. Specification of the simulation model

Ecology. We consider a heterogeneous environment consisting of two habitats (denoted A and B). Individuals settle in one of the habitats at the start of their lives. The viability of an individual in habitat h ($h = A$ or B) is directly proportional to its ecological performance q_h , which depends on the match between the individual's ecological trait x and the optimal strategy μ_h for the habitat. Specifically, $q_h(x) = \exp[-(x - \mu_h)^2 / (2\sigma^2)]$. The parameter σ represents an inverse measure of the intensity of stabilizing selection within habitats. For simplicity, we assume that the intensity of stabilizing selection is identical in the two habitats and that both habitats can support an equal number of individuals. This symmetry is, however, not essential to our conclusions (Fig. S3).

Non-random mating. After viability selection has occurred, females select a mate within their habitat based on a male ornament that acts as a revealing indicator for ecological performance. The mating system is polygynous; the probability that a given female mates with a particular male is proportional to $\exp(\alpha p s)$, where p measures the female's choosiness and s measures the size of the male's ornament (17). The parameter α measures the strength of sexual selection.

Ornament size is affected by the male's mating strategy t , which determines the allocation of resources to expression of the ornament, and by the total amount of resources for reproductive investment $R(q_h)$ available to the male. We take $s = t R(q_h)$ to implement that the ornament is a revealing indicator. This means that males can increase their attractiveness by allocating additional resources to ornament expression (i.e., by increasing t), but for a given level of investment t , high-quality males (i.e., males with high $R(q_h)$) can produce a more attractive ornament than males that have fewer resources available for reproduction. To capture the condition-dependent expression of the ornament, $R(q_h)$ is taken proportional to ecological performance. The proportionality constant can be absorbed into the parameter α , so that we can choose

$s = t q_h$. Male ornament production and female choosiness are costly: male and female survival until reproductive age are reduced by a factor $\exp(-\beta t^2)$ and $\exp(-\gamma p^2)$, respectively. Throughout, we took $\beta = 1.0$, $\gamma = 0.02$.

Density regulation and dispersal. At the end of the generation, the adults in each habitat produce a fixed total number of 2500 offspring per habitat (i.e., selection is ‘soft’; 21). Before the next cycle of selection and mate choice is started, a fraction m of the offspring enters a migrant pool, which is subsequently distributed randomly over the two habitats. Accordingly, the per-capita migration rate between habitats equals $m/2$ per generation.

Genetics and initial conditions. We explicitly model the genetics of the characters x , p and t , such that the mean trait values, the genetic variances and the covariances between characters are free to evolve. Each of the characters is separately encoded by $L = 20$ haploid loci. All loci recombine freely, within and between traits. We assume two alleles per locus. Mutations between alleles occur with a frequency $u = 1 \cdot 10^{-5}$ per allele per generation, and have a phenotypic effect of magnitude $\delta x = 0.1$, $\delta p = 0.05$ and $\delta t = 0.1$ for x , p and t , respectively; the mutational effect sizes δp and δt were chosen in accordance with the different scales of measurement of female choosiness and male ornament investment, which, in turn, are set by our choice of the parameters α , β and γ . The alleles have additive effects on the phenotype, which were chosen such that the ecological character x ranged from $-L \delta x/2$ to $+L \delta x/2$. The mating traits could take only positive values, i.e., p and t ranged from 0 to $L \delta p$ and $L \delta t$, respectively. All simulations were started with genetically monomorphic populations, thus minimizing the amount of genetic variation initially present in the population. We also started all simulations with randomly mating populations, by setting $p = t = 0$ initially.

Speciation criterion. To enable quantitative analysis of our individual-based simulations we use a simple operational species definition that is based on the observed distribution of ecological traits in our simulations. Every generation, we determined the median value of the ecological trait and calculated the mean and standard deviation of the ecological traits above and below the median value separately. We regarded the two artificial

subpopulations thus created as different species if their mean ecological trait values were significantly different from each other based on a t-test at the 0.001 significance level. Based on this criterion, the waiting-time to speciation is defined as the moment at which the overlap between the ecological trait distributions of different species falls below 0.1% for the first time since the start of the simulation. We use the same criterion to test for speciation in the analytical approximation of the simulation model (section 2 of this supplementary online material; Fig. S2), by examining the overlap between equilibrium phenotype distributions of the ecological trait that are obtained in the process of calculating the selection gradients on the mating traits.

Ecological selection regime. To characterize the selection pressures that arise in our ecological model (in the absence of sexual selection) we examine the shape of the fitness landscape $w(x)$. If the genetic variation in the population is small or, alternatively, if selection is weak, $w(x)$ can be approximated by considering the fate of a mutant with ecological strategy x in a population with average strategy \bar{x} . As long as the mutant is rare, its distribution $\vec{\varepsilon}_t = (\varepsilon_A, \varepsilon_B)^T$ across the two habitats A and B changes from generation t to $t+1$ according to the linear equation $\vec{\varepsilon}_{t+1} = \mathbf{M} \vec{\varepsilon}_t$. The transition matrix \mathbf{M} is given by

$$\mathbf{M} = \begin{pmatrix} 1 - \frac{m}{2} & \frac{m}{2} \\ \frac{m}{2} & 1 - \frac{m}{2} \end{pmatrix} \begin{pmatrix} \frac{q_A(x)}{q_A(\bar{x})} & 0 \\ 0 & \frac{q_B(x)}{q_B(\bar{x})} \end{pmatrix}. \quad (1)$$

The first matrix on the right-hand side captures the redistribution of mutant individuals as a result of migration between habitats; the second one captures the change of mutant densities due to selection within each habitat. The function $q_h(x)$ ($h = A$ or B) is given by $q_h(x) = \exp[-(x - \mu_h)^2 / (2\sigma^2)]$, where μ_h is the optimal phenotype in habitat h . The fitness of a rare mutant $w(x)$ can be defined as the geometric rate of increase of the mutant's density, which is given by the dominant eigenvalue of \mathbf{M} .

The actual expression for $w(x)$ is complicated (SI), but its derivatives at $x = \bar{x}$, which characterize the selection regime, evaluate to simple expressions. In particular, the

selection gradient $w'(\bar{x}) = (\mu_A + \mu_B - 2\bar{x}) / (2\sigma^2)$ indicates that the population experiences directional selection until the population mean has converged to the mean of the habitat-specific optima $(\mu_A + \mu_B) / 2$. The curvature of the fitness function $w''(\bar{x})$ at that point indicates whether selection is stabilizing ($w'' < 0$) or disruptive ($w'' > 0$). We find

$$w''\left(\frac{\mu_A + \mu_B}{2}\right) = \frac{1}{\sigma^2} \left(\frac{2-m}{m} \left(\frac{\mu_A - \mu_B}{2\sigma} \right)^2 - 1 \right). \quad (2)$$

Accordingly, selection on the ecological strategy is disruptive when

$$\frac{m}{2-m} < \left(\frac{\mu_A - \mu_B}{2\sigma} \right)^2. \quad (3)$$

From these results, it follows that the intensity of disruptive selection increases with (1) reduced migration between habitats, (2) larger differences between habitat-specific optima and (3) stronger selection for habitat specialization within each habitat (i.e., smaller values of σ). Selection is stabilizing for parameter combinations that violate inequality (3) (the grey area in Fig. 3A extends over such parameter combinations).

In these calculations, we have not accurately dealt with the genetics of the ecological character, nor have we accounted for the fact that the amount of genetic variation that is maintained in the population may be considerable. These issues become problematic if, for example, we aim to predict at what intensity of disruptive selection the population will evolve a bimodal phenotype distribution. A more detailed calculation that fully incorporates the genetics of the character under disruptive selection is required in such a case. Nevertheless, Eq. (2) allows for a classification of ecological selection regimes as either stabilizing or disruptive, and it provides a useful benchmark to estimate selection intensities generated under different parameter settings.

2. Calculation of the selection gradients on choosiness and ornamentation

In order to be able to study the evolutionary dynamics of our model in more detail, we developed a deterministic approximation of our stochastic individual-based simulation model. We are specifically interested in the evolution of the mating traits when the ecological trait is subject to disruptive selection, and the following results apply only to that case. To develop the approximation we combine the hypergeometric model (*S2*, *S3*) with methods from adaptive dynamics (*S4*, *S5*).

Hypergeometric model for the ecological trait. If the population experiences disruptive selection on the ecological trait, it quickly attains a state where a large number of ecological trait loci become polymorphic. In sufficiently large populations, where the loss of alleles due to stochastic fluctuations may be ignored, the number of polymorphic loci depends on the phenotypic effects of individual alleles, and the difference between the ecologically optimal traits in the two habitats. In what follows, we assume that each of the L loci coding for the ecological trait, segregates for two alleles (denoted as + and -) with phenotypic effects of magnitude $+\delta x/2$ and $-\delta x/2$, respectively. As in our individual-based simulations, we chose $\mu_A = -\mu_B = 1$.

As long as $L \delta x \leq |\mu_A - \mu_B|$, the population will tend to evolve to a state where all ecological trait loci are polymorphic and where the allele frequencies across the ecological loci are equal. In this state, all possible genotypes within each particular phenotype class have the same frequency, such that the phenotype distribution is sufficient to keep track of the state of the population (*S2*).

Our choice of the allelic effect sizes relative to the ecological optima μ_A and μ_B , and the assumption that both habitat types are equivalent (they support the same number of individuals and selection is equally strong in both habitats) simplifies our calculations: the assumptions induce a symmetry that only requires us to keep track of the distribution of phenotypes in one of the two habitats. Let f_i denote the distribution of phenotypes among the offspring produced in habitat *A* at the end of a generation, where phenotype classes are indexed by the number of + alleles i ($i \in 0 \dots L$). The distribution of

phenotypes in habitat B is then given by f_{L-i} . Individual-based simulations confirm that the symmetry in our model specification is not essential for our conclusions (Fig. S3). Asymmetric cases can be dealt with in our deterministic approximation at the cost of greater notational complexity, which we choose to avoid here. Our aim is to derive an equation for the change of f_i from one generation to the next. We proceed in three steps to model migration, viability selection and mate choice. For the moment, we will assume that the population is genetically monomorphic for female mating preference and male ornament investment.

At the start of a new generation the phenotype distribution in habitat A changes due to the immigration of individuals from habitat B . The phenotype distribution after migration, f'_i , is given by

$$f'_i = \left(1 - \frac{m}{2}\right) f_i + \frac{m}{2} f_{L-i}. \quad (4)$$

Viability selection then changes the phenotype frequencies in females and males according to

$$f''_i = \frac{w_i f'_i}{\bar{w}}, \quad (5)$$

where the viability of phenotype i is

$$w_i = q_A(x_i) = \exp\left(-\frac{1}{2}\left(\frac{x_i - \mu_A}{\sigma}\right)^2\right), \quad (6)$$

with $x_i = (i - L/2)\delta x$. The average viability \bar{w} in Eq. (5) is defined as $\bar{w} = \sum_i f'_i w_i$.

To calculate the phenotype distribution in the offspring after sexual reproduction, we first define a_i , the attractiveness of males with phenotype i , as

$$a_i = \exp(\alpha p t w_i). \quad (7)$$

To calculate f'''_i , the distribution of offspring phenotypes after mate choice and sexual reproduction, we use the hypergeometric model (S2, S3). Unlike in the individual-based simulations, we will assume haploid genetics to simplify the calculations (S6). Let us

focus initially on a mating pair consisting of a male with $j +$ alleles and a female with $k +$ alleles. The frequency $M_{j \times k}$ of such mating pairs, after mate choice, is given by

$$M_{j \times k} = f_j'' f_k'' \frac{a_j}{\bar{a}}, \quad (8)$$

where $\bar{a} = \sum_i f_i'' a_i$ denotes the average male attractiveness. The phenotype distribution of the offspring produced by the pair follows a binomial distribution over a range that is determined by the parental phenotypes. Suppose, for example, that there are l loci at which the male and female in the mating pair both carry a $+$ allele. At each of these loci, the offspring is bound to inherit a $+$ allele, from either its mother or its father. Summed over the maternal and paternal genome, exactly $j + k - 2l +$ alleles are distributed over the remaining $L - l$ loci where male and female do not both carry a $+$ allele. Each one of these alleles is transmitted to the offspring with a probability of one half. Accordingly, for a given value of l , the probability that the offspring inherits $i +$ alleles follows a binomial distribution

$$B_{j,k,l}(i) = \binom{j+k-2l}{i-l} \left(\frac{1}{2}\right)^{j+k-2l}. \quad (9)$$

Within mating pairs of individuals with phenotypes j and k , l can take a range of values. Obviously, l cannot exceed the minimum of j and k , it has to be non-negative and cannot be smaller than $j + k - L$. With these conditions, and due to the fact that all genotypes within a phenotype class are equiprobable, the value of l within mating pairs with phenotypes j and k follows a hypergeometric distribution,

$$H_{j,k}(l) = \frac{\binom{j}{l} \binom{L-j}{k-l}}{\binom{L}{k}}. \quad (10)$$

The denominator in this expression represents the number of distinct maternal genotypes in phenotype class k . The numerator counts how many of these are compatible with a given value of l . There are j over l ways to ensure that the maternal genotype has $+$ alleles at l loci out of the j in the paternal genotype with $+$ alleles. For each of these

ways, there are $L - j$ over $k - l$ ways to distribute the remaining + alleles in the maternal genotype over loci at which the male does not carry a + allele.

The population distribution of offspring phenotypes after mate choice and sexual reproduction can now be found simply by summing over all possible combinations of parental phenotypes and, given j and k , over the possible values of l , i.e.,

$$f_i''' = \sum_{j=0}^L \sum_{k=0}^L M_{j \times k} \sum_{l=\max(0, j+k-L)}^{\min(j,k)} H_{j,k}(l) B_{j,k,l}(i). \quad (11)$$

With the production of offspring we have arrived at the start of the new generation, which completes the life cycle.

Adaptive dynamics of sexual characters. The sexual characters p and t are under directional or stabilizing selection, so their evolution cannot be studied by the same approach as the one used for the ecological trait. Instead, we rely on an adaptive dynamics approximation. In the individual-based simulations, the female preference and male ornament investment were modeled as multilocus characters. Here, we will deal with these traits as if they were continuous characters. This allows us to calculate the selection gradient for each trait,

$$G_p(p,t) = \left. \frac{\partial \lambda(p',t,p,t)}{\partial p'} \right|_{p'=p} \quad \text{and} \quad G_t(p,t) = \left. \frac{\partial \lambda(p,t',p,t)}{\partial t'} \right|_{t'=t}. \quad (12)$$

The function $\lambda(p',t',p,t)$ is the invasion fitness function ($S4$), which defines the geometric rate of increase of a population of rare mutants with mating trait values p' and t' interacting with resident individuals with the trait values p and t . As indicated by Eq. (12) we always consider mutants that differ from the resident in only one of the mating traits.

The origin of novel advantageous alleles by mutation may eventually lead to a change of resident trait values, if the mutant alleles succeed to invade and replace the resident alleles. Only mutant alleles with positive invasion fitness can invade, and it can be shown that repeated mutation and trait-substitution events lead to evolutionary change of the

mating traits in the direction of the selection gradient. In fact, the long-term evolutionary dynamics of the mating traits can be described by a system of differential equations (S5)

$$\begin{cases} \frac{dp}{d\tau} = k_p G_p(p,t) \\ \frac{dt}{d\tau} = k_t G_t(p,t) \end{cases}, \quad (13)$$

where τ is evolutionary time. We use the rate constants k_p and k_t to scale the evolutionary rates of change of female preference and male ornament investment relative to each other without presently concerning ourselves with the absolute scaling of the evolutionary time τ relative to the generation time in the individual-based simulations. To be precise, we take

$$k_p = \begin{cases} \delta p^2 \left(1 - \frac{p}{L \delta p}\right) & \text{if } G_p(p,t) \geq 0 \\ \delta p^2 \frac{p}{L \delta p} & \text{if } G_p(p,t) < 0 \end{cases}, \quad (14)$$

$$k_t = \begin{cases} \delta t^2 \left(1 - \frac{t}{L \delta t}\right) & \text{if } G_t(p,t) \geq 0 \\ \delta t^2 \frac{t}{L \delta t} & \text{if } G_t(p,t) < 0 \end{cases}.$$

This accounts for the fact that in our individual-based simulations, (1) the mutational variances are different for female preference and male ornament investment, and (2) the rate of evolution upward (or downward) scales with the number of – alleles that could still mutate to a + allele (or vice versa).

We used an iterative procedure to numerically solve the system of differential Eqs. (13). At each step, we consider the frequency distributions of ecological trait phenotypes for the current resident, for a rare female preference mutant and for a rare male trait mutant. The dynamical equations for these frequency distributions (specified below) are iterated until the resident and mutant populations have converged on a stable phenotype distribution. At that point, we evaluate the geometric rate of increase of the mutant population densities, from which we numerically calculate the selection gradients. Using

straightforward Euler integration, the mating traits are then changed by a small amount as specified by Eqs. (13). This completes a single step in the iteration. The iterative procedure terminates when the resident mating trait values have converged on a stable evolutionary equilibrium at which the selection gradients vanish.

The dynamics of ecological trait phenotype frequencies within rare mutant populations. As long as a mutant is rare, its effect on the dynamics of the resident phenotype frequencies can be ignored; the resident frequency distribution then changes from one generation to the next exactly as described above by Eqs. (4) to (11). Slightly modified equations are required to model the mutant populations. Let g_i denote the frequency distribution of ecological types among mutant offspring produced in habitat A at the end of a generation. The mutant has mating traits p' and t' , resident individuals have mating traits p and t . Note that, in the numerical calculations, we always dealt with female preference and male ornament investment mutants separately. Equations for these two types of mutants can be recovered from the results below by substituting $t' = t$ or $p' = p$, respectively.

Exactly as for the resident population, the phenotype distribution in the mutant population after migration, g'_i , is given by

$$g'_i = \left(1 - \frac{m}{2}\right) g_i + \frac{m}{2} g_{L-i}. \quad (15)$$

Viability selection changes the phenotype frequencies in mutant females and males according to

$$g''_i = \frac{w_i g'_i}{\bar{w}}. \quad (16)$$

Since the mutant can be assumed to be rare, the average viability \bar{w} is fully determined by the phenotype distribution in the resident population, i.e., $\bar{w} = \sum_i f'_i w_i$, as for the resident.

To calculate the phenotype distribution in mutant offspring after sexual reproduction, we define a_i^M , the attractiveness of mutant males with phenotype i as perceived by resident females,

$$a_i^M = \exp(\alpha p' t' w_i). \quad (17)$$

In addition, we define a_i^F , the attractiveness of resident males with phenotype i as perceived by mutant females,

$$a_i^F = \exp(\alpha p' t w_i). \quad (18)$$

It is necessary to consider two types of mutant mating pairs: either the male or the female in the pair could be a mutant individual (since we focus on a rare mutant, mating interactions between mutants are so rare that they can be ignored). The frequency of mating pairs consisting of a mutant male with $j +$ alleles and a resident female with $k +$ alleles, is given by

$$M_{j \times k}^M = f_k'' \frac{g_j'' a_j^M}{\bar{a}}, \quad (19)$$

where $\bar{a} = \sum_i f_i'' a_i$, exactly as earlier for the resident population. The frequency of pairs with a female mutant individual, is given by

$$M_{j \times k}^F = g_k'' \frac{f_j'' a_j^F}{\sum_j f_j'' a_j^F}. \quad (20)$$

Note that the expression on the right-hand side is normalized by the average attractiveness of resident males as perceived by mutant females. This ensures that mutant females mate as often as resident females irrespective of their mating preference.

The population distribution of mutant offspring phenotypes after mate choice and sexual reproduction is found in a manner analogous to that detailed for the resident population,

$$g_i''' = \frac{1}{2} \sum_{j=0}^L \sum_{k=0}^L (M_{j \times k}^M + M_{j \times k}^F) \sum_{l=\max(0, j+k-L)}^{\min(j,k)} H_{j,k}(l) B_{j,k,l}(i). \quad (21)$$

The factor of one half in front of the right-hand side of this expression accounts for the fact that only half of the offspring from a mutant mating pair will inherit the mutant allele from its mutant parent.

Numerical fitness calculations. Unlike the recurrence for the resident population (Eqs. (4) to (11)), the dynamical equations for the mutant population (Eqs. (15) to (21)) do not

conserve the total number of mutant individuals. After an initial phase, during which the phenotype distribution in the mutant population attains a stable shape, the total number of mutant individuals, $\sum_i g_i$, will either increase or decrease geometrically. In fact, the geometric rate of increase of the mutant population provides a measure for the mutant's invasion fitness $\lambda(p', t', p, t)$ (S4).

Phase-space analysis. Our analytical approximation is amenable to many of the numerical techniques that have been developed for the analysis of systems of differential equations, with as only practical limitation that obtaining accurate numerical solutions of our model is computationally demanding. Fig. S2 provides an example of a standard qualitative phase-space analysis: the trajectory was calculated using a straightforward Euler integration routine, and the null-isoclines were found using the bisection method for root finding.

Fig. S2 shows results for the same parameters as in Fig. 2 in the main text. As in the individual-based simulation, the distribution of ecological phenotypes is unimodal in a population that mates randomly (compare Fig. 2A and Fig. S2, inset A). However, the equilibrium at $p = t = 0$ is unstable. Sexual selection drives the population away from random mating towards increased levels of choosiness by females and increased investment of resources into expression of the condition-dependent ornament by males. A stable equilibrium is reached at $p = 0.59$ and $t = 1.44$, where the combined strength of sexual and ecological disruptive selection has exceeded the level that is required for speciation. Along the evolutionary trajectory, the ecological phenotype distribution changes from unimodal to strongly bimodal, exactly as observed in the individual-based simulations. In fact, the stochastic trajectories of different simulations closely follow the deterministic prediction, providing confidence in the accuracy of the approximation. The deterministic trajectory initially closely follows the t -isocline, but departs from that isocline in the area where the ecological phenotype distribution changes from unimodal to bimodal (between points B and C). This signifies a transition from weak to strong selection on choosiness at a crucial stage during the speciation process that results from a positive feedback between the effectiveness of sexual selection and ecological divergence.

3. Figures

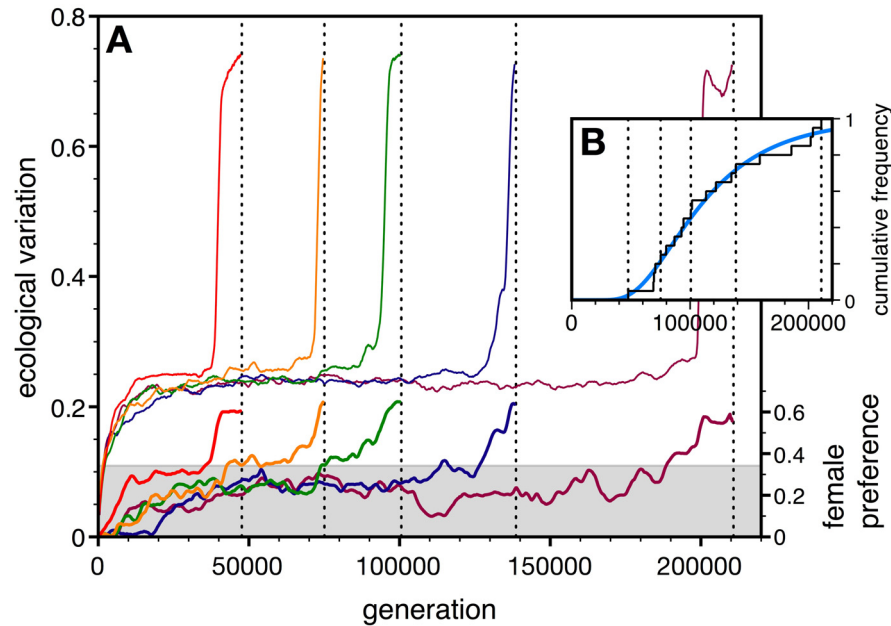


Fig. S1. Replicate simulations. (A) Five replicate simulations (represented by different colours) show variation in the waiting time to speciation. In all cases, speciation occurs rapidly after the female preference (thick lines) first exceeds a critical threshold level (indicated by the grey area). Speciation is accompanied by a sudden increase of the variability of ecotypes (thin lines show the standard deviation of the ecological character). The associated increase in the variability of male attractiveness, mediated by condition-dependent expression of the ornament, provides increased benefits to choosiness and generates a positive feedback between the effectiveness of mate choice and ecological diversification. Dotted lines indicate for each of the replicates when the speciation criterion was met. (B) The cumulative distribution of the waiting time to speciation (black line) based on the 5 simulations shown in (A) and 15 additional replicates, fits well with the distribution of waiting times for a biased random walk process (light-blue curve), suggesting that selection on choosiness during the initial phase of the simulations is weak and dominated by random drift (see also Fig. S2). Parameters are: $\mu_A = 1$, $\mu_B = -1$, $\sigma = 0.8$, $m = 1$, $\alpha = 5.0$, $\beta = 1.0$, $\gamma = 0.02$.

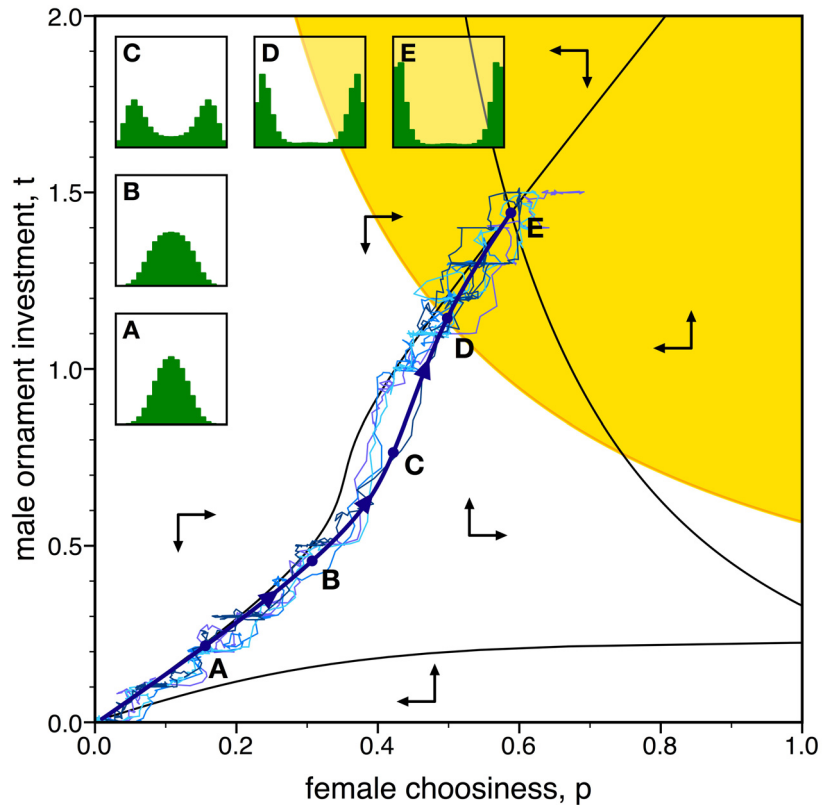


Fig. S2. Evolution of the mating traits. Evolutionary equilibria are located at the intersections of black null-isoclines, which separate the phase-space into regions differing in expected directions of evolutionary change (arrows). For sufficiently high values of p and t , sexual selection is strong enough to induce speciation (yellow area). In a randomly mating population ($p = t = 0$) speciation does not occur, due to the lack of reproductive isolation between habitat specialists. However, sexual selection pushes the population along the blue trajectory towards a stable equilibrium within the speciation region. Five insets show the frequency distribution of the ecological character at the points **A** – **E** along the trajectory. At equilibrium, the ecological trait distributions of the two species overlap less than 0.5%. The stochastic trajectories from four replicate individual-based simulations (thin blue lines) follow the deterministic trajectory and converge to the same equilibrium point. Parameters as in Fig. 2.

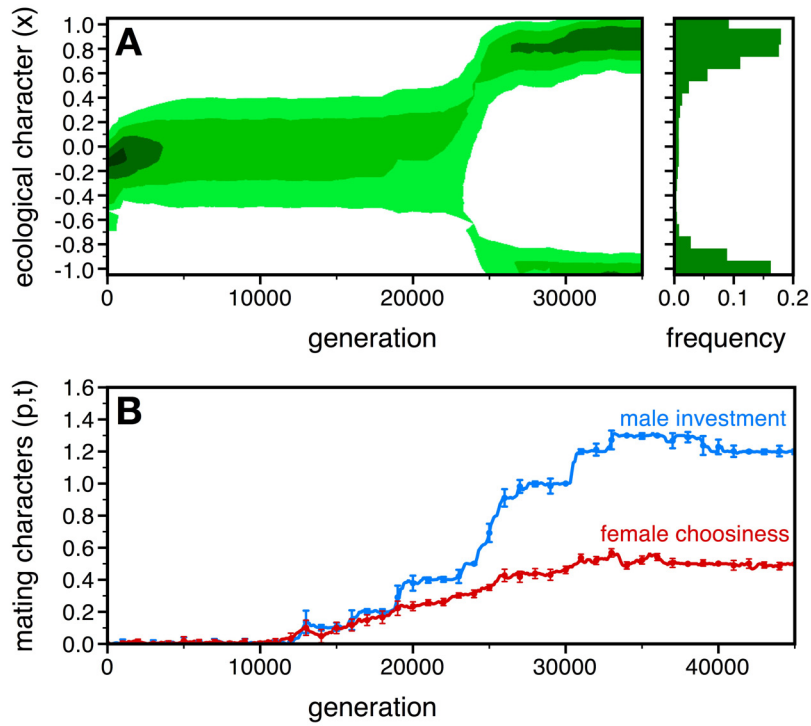


Fig. S3. Speciation under resource asymmetry. The simulations in the main text present results for two habitats that have different optima but are otherwise equivalent. As indicated by this simulation run, our main conclusions are not sensitive to this symmetry. (**A**, **B**) Speciation can occur also when the two patches have different carrying capacities and when the intensity of selection differs between habitats. In this run, habitat A and B supported, respectively, 3500 and 1500 individuals, and we took $\sigma_A = 1$ and $\sigma_B = 0.6$. Other parameters are as in Fig. 2.

4. Supporting references and notes

- S1. O. Leimar. *Am. Nat.* **165**, 669–681 (2005).
- S2. M. Shpak, A.S. Kondrashov. *Evolution* **53**, 600-604 (1999).
- S3. N.H. Barton, M. Shpak. *Theor. Pop. Biol.* **57**, 249–263 (2000).
- S4. S. A. H.Geritz, É Kisdi, G. Meszéna, J.A.J. Metz. *Evol. Ecol.* **12**, 35-57 (1998).
- S5. U. Dieckmann, R. Law. *J. Math. Biol.* **34**, 579–612 (1996).
- S6. With additive genetics, this difference is inconsequential. If desired, our approach can be extended; the hypergeometric model can deal with diploid genetics.